Journal of Molecular Liquids 203 (2015) 111–119

Contents lists available at ScienceDirect

Journal of Molecular Liquids

journal homepage: www.elsevier.com/locate/molliq

Carvone Schiff base of isoniazid as a novel antitumor agent: Nanoemulsion development and pharmacokinetic evaluation

Mashooq A. Bhat [a], Muzaffar Iqbal [a,b], Abdullah Al-Dhfyan [c], Faiyaz Shakeel [d,*]

[a] Department of Pharmaceutical Chemistry, College of Pharmacy, King Saud University, P.O. Box 2457, Riyadh 11451, Saudi Arabia
[b] Bioavailability Laboratory, College of Pharmacy, King Saud University, P.O. Box 2457, Riyadh 11451, Saudi Arabia
[c] Stem Cell & Tissue Re-Engineering Program, Research Center, King Faisal Specialized Hospital & Research Center, MBC-03, P.O. Box 3354, Riyadh 11211, Saudi Arabia
[d] Center of Excellence in Biotechnology Research (CEBR), College of Science, King Saud University, P.O. Box 2460, Riyadh 11451, Saudi Arabia

ARTICLE INFO

Article history:
Received 16 December 2014
Received in revised form 25 December 2014
Accepted 26 December 2014
Available online 30 December 2014

Keywords:
Isoniazid schiff base
Nanoemulsion
Cytotoxicity
Droplet size
Pharmacokinetic

ABSTRACT

In the present study, various nanoemulsion formulations of carvone Schiff base of isoniazid (CSB-INH) were developed by aqueous phase titration method in order to evaluate its anticancer potential. Developed nanoemulsions of CSB-INH were characterized in terms of thermodynamic stability, self-nanoemulsification efficiency, droplet size, polydispersity index (PI), zeta potential (ZP), viscosity, refractive index (RI), % transmittance (% T), surface morphology and in vitro drug release studies. Based on lowest droplet size (19.4 nm), least PI (0.189), lowest viscosity (29.6 cP), optimal values of ZP (−30.8 mV) & RI (1.341), highest % T (98.9%), highest drug release profile (94.5% after 24 h) and the presence of lowest concentration of Triacetin (12% w/w), formulation N1 was selected for in vitro cytotoxicity and in vivo pharmacokinetic studies. Cytotoxicity studies on human colon cancer cells indicated that CSB-INH in optimized nanoemulsion is around nine times more efficacious than free CSB-INH. Pharmacokinetic studies in Albino rats showed rapid absorption (rate and extent) of CSB-INH from optimized nanoemulsion as compared to its suspension formulation. These results indicated the potential of developed nanoemulsion for oral delivery of CSB-INH for chemoprevention of colon cancer.

1. Introduction

Colon cancer has been reported as the third most common tumor among various tumors [1]. In the recent years, the incidence of colon cancer has been increased gradually, hence its treatment become a focus of research around the globe [2–4]. Radiation therapy, surgery and chemotherapy are the three commonly used modalities for the cure and control of colon cancer [5]. In chemotherapy, the anticancer drug 5-fluorouracil is the commonly used drug for the treatment of colon cancer [1,5]. Recently, Bhat and Al-Omar (2013) synthesized and investigated various terpene Schiff bases of anti-tubercular drug isoniazid (INH) for the effective treatment of tuberculosis [6]. Among various terpene Schiff bases investigated, the carvone Schiff base of INH (CSB-INH) was found to be very potent and effective. Moreover, various hydrazines, hydrazones, nicotinic acid and terpene derivatives of INH have also been investigated successfully for the treatment of various cancers such as colon cancer, ovarian cancer, blood cancer, glioblastoma and tuberculosis [1,6–12]. Therefore, in the present study, CSB of INH was synthesized, characterized and investigated for its anticancer potential in the form of nanoemulsion. Previously, CSB-INH was found to be most effective against *Mycobacterium tuberculosis*, hence it was selected in the present investigation [6]. Recently, nanotechnology-based drug delivery systems have been investigated effectively for the targeting of various anticancer drugs to carcinoma cells in order to enhance therapeutic efficacy and to reduce the adverse effects of the treatment both in vitro as well as in vivo [13–19]. Moreover, various nanocarries have also been investigated as the effective drug delivery vehicles for the targeting of INH and its analogues in order to reduce the dose and adverse effects of the treatment [20–25]. Nanoemulsions are oil/lipid based clear, transparent/isotropic and thermodynamically/thermokinetically stable systems composed of oil/lipid, surfactant and cosurfactant with droplet size in the range of 10–100 nm [13–15]. These novel nanovehicles have been investigated effectively for the multipurpose drug delivery system in order to enhance in vitro dissolution rate/solubility, in vivo therapeutic efficacy and bioavailability of various poorly water-soluble drugs [13–15,26–29]. Nanoemulsion system offers several advantages over unstable dispersions (emulsions, suspensions and colloids) [26]. These advantages include ease of preparation, excellent solubilization capacity, physical stability, smaller droplet size, lower viscosity and bioavailability enhancement [27,28]. CSB-INH is poorly water soluble compound (solubility: 0.11 mg/ml) with log p value of 3.02 [6]. Till date, the antitumor potential of CSB-INH via nanoemulsion approach has not been investigated in the literature so far. Therefore, in the present study, CSB-INH was synthesized

* Corresponding author.
E-mail address: faiyazs@fastmail.fm (F. Shakeel).

http://dx.doi.org/10.1016/j.molliq.2014.12.037
0167-7322/

and characterized in order to investigate its antitumor effects against human colon cancer cell lines.

2. Materials and methods

2.1. Materials

INH, carvone, polyoxy-35-castor oil (Cremophor-EL), ethanol and polyoxyethylene (20) sorbitan monooleate (Tween-80) were purchased from Sigma Aldrich (St. Louis, MO). Glycerol triacetate (Triacetin) was purchased from Alpha Chemica (Mumbai, India). Propylene glycol monocaprylate-type II (Capryol-90), propylene glycol monolaurate-type II (Lauroglycol-90), oleoyl macrogol-6-glyceride (Labrafil-M1944CS), propylene glycol dicaprylocaprate (Labrafac-PG), caprylo caproyl macrogol-8-glyceride (Labrasol) and diethylene glycol monoethyl ether (Transcutol-HP) were kind gift samples from Gattefossé (Lyon, France). Iso-octylphenoxypolyethoxyethanol (Triton-X100), propylene glycol (PG) and polyethylene glycol-400 (PEG-400) were purchased from BDH Laboratories (Liverpool, UK). Chromatographic grade acetonitrile was purchased from BDH Laboratory (Liverpool, UK). HT-29 human colon cancer cell lines were purchased from American type cell culture collection (ATCC, Manassas, VA). Ultrapure water was obtained in the laboratory from ELGA water purification unit (Wycombe, Bucks, UK). All other solvents and reagents used were of LR grade and obtained from E-Merck (Germany).

2.2. Synthesis and characterization of carvove Schiff base of INH

CSB-INH was prepared by the reaction of carvone (0.15 g, 1 mmol) with INH (0.14 g, 1 mmol) in ethanol/water (10 ml). Initially, INH was dissolved in water and the alcoholic solution of carvone was added to the INH solution. This mixture was stirred at room temperature for about 1–3 h and then concentrated under reduced pressure. The residue obtained was purified by washing with cold ethanol and ethyl ether. Colorless blocks of compounds were prepared by recrystallization with ethanol by the slow evaporation of solvent at room temperature. The synthesized compound was characterized in terms of % yield, melting point, FTIR, ^{1}H NMR, ^{13}C NMR, mass spectra and elemental analysis [6]. CSB-INH was synthesized according to Scheme 1. The molecular structure of CSB-INH was confirmed by FTIR, ^{1}H NMR, ^{13}C NMR, mass spectra and elemental analysis. This compound was successfully investigated as a potential anti-tubercular agent in previous studies [6]. In the present study, its potential as a potent anti-tumor agent against human colon cancer cell line was investigated.

2.3. Screening of components for nanoemulsion preparation

The selection of components in terms of oil phase, surfactant and cosurfactant was based on the solubility of CSB-INH. Therefore, the saturated solubility of CSB-INH in different oils (Triacetin, Capryol-90, Lauroglycol-90, Labrafac-PG and Labrafil-M1944CS), different surfactants (Tween-80, Labrasol, Cremophor-EL and Triton-X100), different cosurfactants (Transcutol-HP, PEG-400, PG and ethanol) and water was determined by adding the excess amount of CSB-INH in 2 ml of each component in 5 ml capacity vials. All the mixtures were continuously mixed in an isothermal water shaker bath (Julabo, MA) at 100 rpm and 37 ± 0.5 °C for 72 h [26,28]. After 72 h, each mixture was taken out from the shaker bath and centrifuged at 5000 rpm for 20 min, and the supernatant was diluted suitably with methanol and subjected for analysis of CSB-INH content spectrophotometrically at 220 nm.

2.4. Construction of pseudo-ternary phase diagrams

Based on highest solubilization potential of CSB-INH, Triacetin, Tween-80 and Transcutol-HP were used as oil phase, surfactant and cosurfactant, respectively for the development of nanoemulsions. Deionized water selected as an aqueous phase. For the construction of pseudo-ternary phase diagrams, Surfactant (Tween-80) and cosurfactant (Transcutol-HP) were mixed in various mass ratios (1:0, 1:2, 1:1, 2:1 and 3:1). Triacetin (oil phase) and a particular mass ratio of Tween-80 to Transcutol-HP (S_{mix}) were mixed at mass ratios of 1:9 to 9:1. Pseudo-ternary phase diagrams were developed by titrating the mixture of oil phase and specific S_{mix} slowly with deionized water (aqueous phase titration method) [28,29]. The physical state of nanoemulsions was marked on a phase diagram with the first axis representing the aqueous phase (water), second oil phase (Triacetin) and third representing the specific mass ratio of surfactant (Tween-80) to cosurfactant (Transcutol-HP).

2.5. Formulation development

The maximum nanoemulsion zones were observed in 1:1 mass ratio of Tween-80 and Transcutol-HP, hence this ratio was selected for the preparation of CSB-INH nanoemulsions. From the pseudo-ternary phase diagram, different nanoemulsions with formulation codes of N1–N5 were selected (Table 1). Almost the entire range of nanoemulsion zones in the phase diagram were taken into account and varied Triacetin compositions (12, 16, 20, 24 and 28% w/w) with minimum Tween-80 (12% w/w) and Transcutol-HP (12% w/w) concentration were selected. 25 mg of CSB-INH was directly solubilized in each nanoemulsion by vortexing at 1000 rpm and 25 ± 1 °C for about 5 min. After 5 min, the drug was completely solubilized in the system and CSB-INH-loaded nanoemulsions were transferred into transparent glass vials (Table 1).

2.6. Thermodynamic stability and self-nanoemulsification tests

Thermodynamic stability tests on prepared CSB-INH nanoemulsions were carried out in order to remove unstable or metastable nanoemulsions. These tests were performed in terms of centrifugation (at 5000 rpm for 30 min), heating & cooling cycles (3 cycles between 4 and 50 °C for 48 h) and freeze–pump–thaw cycles (3 cycles between −21 and +25 °C for 24 h) as reported in the literature [28,29]. The objective of the self-nanoemulsification efficiency test was to evaluate any phase separation or precipitation upon dilution with water. In order to perform this test, 1 ml of each CSB-INH nanoemulsion (N1–N5) was diluted 500 times with deionized water. The efficiency of each nanoemulsion was evaluated visually using the following A–E grading systems as reported previously [26,29]:

Grade A: Rapid forming clear/translucent nanoemulsion
Grade B: Rapid forming bluish slightly less clear nanoemulsion
Grade C: Slowly forming milky/turbid emulsions
Grade D: Dull, grayish slowly forming milky emulsions
Grade E: Emulsions with oil globules at the surface.

2.7. Physicochemical characterization of CSB-INH nanoemulsions

Prepared CSB-INH nanoemulsions were characterized physicochemically in terms of droplet size distribution, polydispersity index (PI), zeta potential (ZP), viscosity, refractive index (RI), percentage of transmittance (% T) and transmission electron microscopy (TEM). The mean droplet size, PI and ZP of CSB-INH nanoemulsions (N1–N5) were recorded using Malvern Particle Size Analyzer/Zetasizer (Malvern Instruments Ltd., Holtsville, NY) at room temperature at a scattering angle of 90° as reported previously [30]. The viscosity and RI of CSB-INH nanoemulsions (N1–N5) were recorded using Brookfield Viscometer (Brookfield Engineering Laboratories, Middleboro, MA) and Abbes type Refractometer (Precision Testing Instruments Laboratory, Germany) at 25 ± 1 °C, respectively as reported in the literature [28, 29]. The % T of CSB-INH nanoemulsions (N1–N5) was recorded

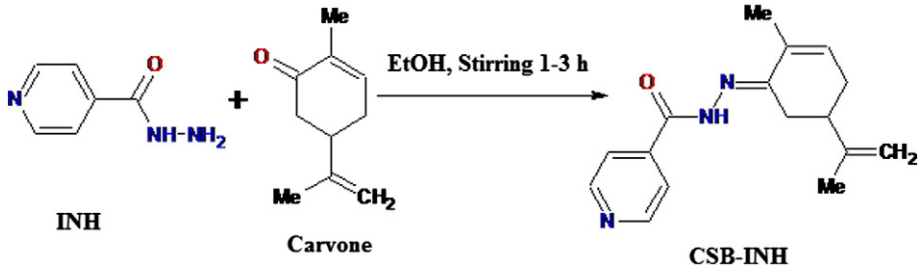

Scheme 1. Synthesis of CSB-INH.

spectrophotometrically at the wavelength of 550 nm as reported previously [29].

TEM analysis (Tecnai TF20, Hillsboro, OR) was performed to evaluate the surface morphology of droplets of optimized nanoemulsion N1. TEM analysis was performed under light microscopy operating at 200 kV as reported previously [26].

2.8. In vitro drug release studies

In vitro drug release studies on CSB-INH nanoemulsions (N1–N5) were performed to compare the release profile of CSB-INH from different nanoemulsions and CSB-INH suspension, all having the same amount of drug (25 mg). These studies were performed in 500 ml of gastric buffer (pH 1.2) (dissolution media) using USP XXIV method at 100 rpm and 37 ± 0.2 °C [26]. In order to perform these studies, 1 ml each of CSB-INH nanoemulsion (N1–N5) and CSB-INH suspension was placed in a ready-to-use dialysis bag. Three milliliters of samples was withdrawn at regular time intervals of 0, 0.5, 1, 2, 3, 4, 5, 6, 8, 18 and 24 h and the same amount of drug free fresh gastric buffer (pH 1.2) was replaced every time. The samples were analyzed for CSB-INH content spectrophotometrically at 220 nm.

2.9. Kinetic analysis of drug release data

The release mechanism of CSB-INH from developed nanoemulsions was investigated using various kinetic models such as zero order, first order, Higuchi, Hixson–Crowell and Korsemeyer–Peppas models [31,32]. This analysis was performed using Microsoft excel 2010 program. The mathematical representation of these models is as follows:

Zero order

$$Q_t = Q_0 + K_0 t \tag{1}$$

First order

$$\mathrm{Log}\, C = \mathrm{Log}\, C_0 - \frac{K_1 t}{2.303} \tag{2}$$

Higuchi

$$Q_t = kt^{0.5} \tag{3}$$

Hixson–Crowell cube root

$$\left(W_0^{\frac{1}{3}} - W_t^{\frac{1}{3}}\right) = k_h t \tag{4}$$

Korsmeyer–Peppas

$$\frac{Q_t}{Q_\infty} = k_p t^n. \tag{5}$$

2.10. In vitro cytotoxicity studies

With the background to develop a suitable nanoemulsion formulation to investigate the anticancer potential of CSB-INH, we investigated in vitro therapeutic efficacy of optimized nanoemulsion N1 on HT-29 human colon cancer cell line. In vitro cytotoxicity (%) was evaluated by exposing different molar concentrations of CSB-INH from optimized nanoemulsion (N1) and free CSB-INH (aqueous solution). Optimized formulation N1 without CSB-INH was also applied in the same volume as applied for CSB-INH loaded N1 which was used as a control. A WST-1 [2-(4-iodophenyl)-3-(4-nitrophenyl)-5-(2, 4-disulfophenyl)-2H-tetrazolium] assay was performed to assess the cytotoxic effects of CSB-INH nanoemulsion (N1), CSB-INH solution and control. The HT-29 colon cancer cells were cultured in RPMI 1640 medium, supplemented with 10% fetal bovine serum (FBS), 1% ABM (GIBCO), 2 mmol/l of L-glutamine, 100 IU/ml penicillin and 100 mg/ml streptomycin at 37 °C in a 5% CO_2 atmosphere. Cells were seeded into 96-well plates at 0.4×10^4 cells/well and incubated for 24 h in an incubator at 37 °C in a 5% CO_2 atmosphere. The medium was replaced with a fresh one containing the desired concentrations of aqueous solution, nanoemulsion (N1) and control in the same volume. After 72 h, 10 μl of the WST-1 reagent was added to each well and the plates were reincubated for 4 h at 37 °C. The amount of formazan was quantified using ELISA reader at 450 nm.

2.11. Pharmacokinetic study in rats

Twelve male Wistar albino rats weighing 210 ± 15 g (mean ± SD) were obtained from the Animal Care and Use Centre, College of Pharmacy, King Saud University, Riyadh, Saudi Arabia. Prior to the experiment, the animals were acclimatized and kept in plastic cages under standard laboratory conditions, a temperature of 25 ± 2 °C and 55 ± 5% RH with a 12 h light/dark cycle and a pellet diet was given with water ad libitum. All experiments were carried out according to the guidelines of the Animal Care and Use Committee at King Saud University. In a single dose parallel designed study, the rats were randomly divided into two groups (6 in each) which served as CSN-INH suspension and CSB-INH nanoemulsion (N1) treatment group, respectively. The rats were fasted for at least 10 h before the experiments. Blood samples (approximately 0.75 ml) were collected from the retro-orbital plexus into heparinized

Table 1
Composition of CSB-INH nanoemulsions (N1–N5) prepared using Triacetin, Tween-80, Transcutol-HP and water.

Code	Formulation composition (% w/w)[a]				S_{mix} ratio
	Triacetin	Tween-80	Transcutol-HP	Water	
N1	12	12	12	64	1:1
N2	16	12	12	60	1:1
N3	20	12	12	56	1:1
N4	24	12	12	52	1:1
N5	28	12	12	48	1:1

[a] Twenty five milligrams of CSB-INH was incorporated into each nanoemulsion.

microfuge tubes at predose and at 0.5 1, 2, 3, 4, 6, 8 and 24 h after administration of CSB-INH (5 mg/kg, oral) in both groups. Plasma samples were harvested by centrifuging the blood at 45,00 ×*g* for 8 min and stored frozen at −80 ± 10 °C until analysis.

2.12. Determination of CSB-INH concentration in plasma by UPLC MS/MS

The ACQUITY™ UHPLC system coupled to a triple-quadruple tandem mass spectrometer Micromass® Quattro micro™ (Waters Corp., Milford, MA, USA) was used to analyze the CSB-INH in rat plasma samples using carbamazepine as an internal standard (IS). The chromatographic separation was achieved on Acquity BEH™ C_{18} column (50 × 2.1 mm, I.D., 1.7 μm, Waters, USA) maintained at 40 °C. The mobile phase was composed of acetonitrile-10 mM ammonium acetate (95:5,v/v) at a flow rate of 0.3 ml/min. A triple-quadruple tandem mass spectrometer equipped with electrospray ionization (ESI) interface was used for the analytical detection of both analyte and IS. The detection was performed in ESI positive mode using multiple reaction monitoring (MRM) by the ion transitions of m/z 270.08 > 79.93 for CSB-INH and m/z 237.0 > 178.97 for IS, having a dwell time of 0.106 s. The optimized cone voltage and collision energy were 38 V and 32 eV for CSB-INH and 32 V and 34 eV for IS, respectively. The collision gas (argon) flow was 0.1 ml/min and capillary voltage was set at 3.5 kV. The Mass Lynx software (Version 4.1, SCN 714) was used to control the UHPLC-MS/MS system and data was collected and processed using TargetLynx™ program. Samples were prepared by protein precipitation method using acetonitrile (ACN). Plasma samples (200 μl) were transferred to 1.5 ml centrifuge tubes and 20 μl of IS (40 μg/ml in ACN) was added. The samples were vortexed mixed for 20 s and 380 μl of ACN was added. The samples were again vortex mixed gently for 1 min. Samples were centrifuged at 12,500 ×*g* at 8 °C for 10 min. The supernatant was transferred to UPLC vials subjected to 5 μl for the analysis. The proposed analytical method was validated according to the FDA and EMEA guidelines [33].

2.13. Pharmacokinetic calculation and data analysis

The plasma concentrations were used to construct pharmacokinetic profiles by plotting drug concentration–time profile curves. All values are expressed as the mean ± SD. To determine pharmacokinetic parameters, all obtained data were subsequently fed into PK software on Microsoft excel®. The noncompartmental pharmacokinetic parameters such as maximum plasma concentration (C_{max}) and time to reach maximum concentration (T_{max}), area under the curve from 0 to *t* (AUC_{0-24}) and area under first moment curve from 0 to 24 ($AUMC_{0-24}$), elimination rate constant (K_{el}) and half-life were calculated whereas, mean residence time (MRT) is the ratio of $AUMC_{0-24}$ to AUC_{0-24}. Unpaired T-test with two tail P value was used for statistical calculation using GraphpadInstat software.

2.14. Statistical analysis

In vitro drug release data, characterization parameters among CSB-INH nanoemulsions (N1–N5) and in vitro cytotoxicity data were statistically evaluated by one way analysis of variance (ANOVA) using Dennett's test to evaluate the significant differences using GraphpadInstat software. Data were considered statistically significant at the value of $p < 0.05$.

3. Results and discussion

3.1. Screening of components for nanoemulsion preparation

The saturated solubility of drug (CSB-INH) in oils, surfactants and cosurfactants is the most important step for the screening of components especially in oral drug delivery systems [26,28]. Hence, in the present study, these components were screened based on highest solubility of CSB-INH in these components. The saturated solubility data of CSB-INH in different components at 37 °C is listed in Table 2. Among the different oils investigated, the highest solubility of CSB-INH was observed in Triacetin (42.42 ± 3.84 mg/ml) followed by Lauroglycol-90, Capryol-90, Labrafac-PG and Labrafil-M1944CS (Table 2). However, the highest solubility of CSB-INH was observed in Tween-80 (67.24 ± 6.13 mg/ml) among different surfactants followed by Cremophor-EL, Labrasol and Triton-X100. On the other hand, the highest solubility was observed in Transcutol-HP (76.84 ± 7.86 mg/ml) among different cosurfactants investigated followed by ethanol, PEG-400 and PG. CSB-INH was found to be poorly soluble in water (solubility 0.11 mg/ml) as shown in Table 2. Based on the solubility data of CSB-INH, Triacetin, Tween-80 and Transcutol-HP were selected as oil phase, surfactant and cosurfactant, respectively. However, deionized water was selected as aqueous phase.

3.2. Nanophasic map construction and formulation development

Pseudo-ternary phase diagrams were constructed separately for each S_{mix} ratio and the results are presented in Fig. 1. From the phase diagrams, it was observed that S_{mix} 1:0 showed relatively low nanoemulsion zones (Fig. 1A). The highest amount of Triacetin (oil phase) that was solubilized by this ratio was found to be 16% w/w with a high percentage of S_{mix} (64% w/w). However, in the case of S_{mix} 1:2 (Fig. 1B), when the cosurfactant (Transcutol-HP) was used along with Tween-80 (surfactant), the nanoemulsion zones increased rapidly as compared to the previous S_{mix} ratio. The highest amount of oil phase that was solubilized by 1:2 ratio was found to be 22% w/w by incorporating 52% w/w of S_{mix}. On the other hand, when S_{mix} ratio of 1:1 (Fig. 1C) was investigated, the nanoemulsion zones increased significantly as compared to previous ratios (1:0 and 1:2 ratios). The highest amount of oil phase that was solubilized by this ratio was found to be 34% w/w by incorporating lower concentration of S_{mix} (30% w/w). These results showed the dominance of cosurfactant (Transcutol-HP) along with surfactant (Tween-80) in nanosizing. When S_{mix} ratio of 2:1 was investigated (Fig. 1D), the nanoemulsion zones started to decrease as compared to 1:1 ratio. The highest amount of oil phase that was solubilized by 2:1 ratio was found to be 28% w/w by incorporation of 41% w/w of S_{mix}. When S_{mix} ratio of 3:1 was investigated (Fig. 1E), the nanoemulsion zones decreased further as compared to 1:1 and 2:1 ratios. The highest amount of oil phase that was solubilized by 3:1 ratio was found to be 17% w/w by incorporation of 39% w/w of S_{mix}. Phase titration studies showed that the highest nanoemulsion zones were exposed by S_{mix} ratio of 1:1 as shown in Fig. 1C. Therefore, different nanoemulsion compositions were precisely selected from Fig. 1C. Almost the entire nanoemulsion zones in Fig. 1C were covered and different oil compositions (12, 16, 20, 24 and 28%

Table 2
Equilibrium solubility data of CSB-INH in various oils, surfactants and cosurfactants at 37 °C (n = 3).

Sample matrices	Solubility ± SD (mg/ml)
Triacetin	42.42 ± 3.84
Capryol-90	15.24 ± 1.38
Lauroglycol-90	18.62 ± 2.08
Labrafac-PG	8.34 ± 0.81
Labrafil-M1944CS	7.13 ± 0.65
Tween-80	67.24 ± 6.13
Labrasol	32.15 ± 2.65
Cremophor-EL	37.26 ± 3.76
Triton-X100	25.81 ± 2.21
Transcutol-HP	76.84 ± 7.86
PEG-400	28.61 ± 2.52
PG	19.23 ± 1.78
Ethanol	61.23 ± 5.34
Water	0.11 ± 0.00

Polyethylene glycol-400 (PEG-400), propylene glycol (PG).

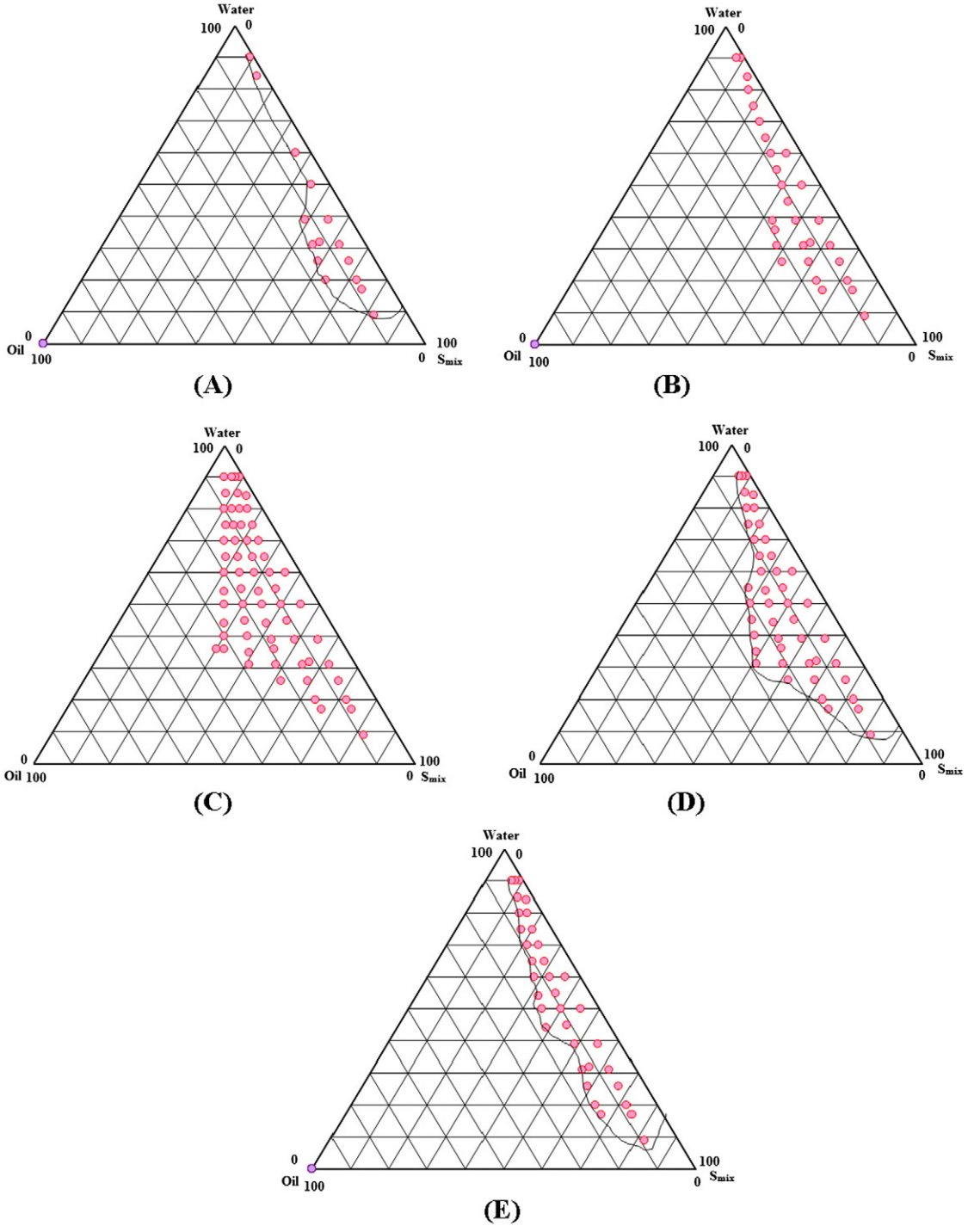

Fig. 1. Pseudo-ternary phase diagrams with nanoemulsion zones (dotted area) for oil phase (Triacetin), aqueous phase (water), surfactant (Tween-80) and cosurfactant (Transcutol-HP) at S_{mix} ratios of A. 1:0, B. 1:2, C. 1:1, D. 2:1 and E. 3:1.

w/w) with fixed S_{mix} concentration (24% w/w) were precisely selected. 25 mg of compound (CSB-INH) was directly encapsulated on each nanoemulsion. The composition of CSB-INH loaded nanoemulsions is listed in Table 1.

3.3. Thermodynamic stability and self-nanoemulsification tests

The objective of thermodynamic stability tests was to eliminate metastable/unstable formulations. In order to develop robust and stable nanoemulsions, developed formulations were subjected to different thermodynamic stability tests. Thermodynamically stable nanoemulsions (N1–N5) were further evaluated for self-nanoemulsification efficiency. The self-nanoemulsification efficiency test showed that formulations N1–N4 passed this test with grade A while the formulation N5 passed this test with grade B.

3.4. Physicochemical characterization of CSB-INH nanoemulsions

The results of physicochemical parameters of CSB-INH nanoemulsions are listed in Table 3. The mean droplet size of CSB-INH nanoemulsions

(N1–N5) was observed in the range of 19.4–124.4 nm (Table 3). The droplet size of prepared nanoemulsions was found to be reduced rapidly by decreasing the concentration of oil phase (Triacetin) in the formulations. The largest droplet size was observed in nanoemulsion N5 (124.4 ± 14.8 nm) which was probably due to the presence of the highest concentration of Triacetin (28% w/w) in N5. However, the droplet size of nanoemulsion N1 was found to be lowest (19.4 ± 2.3 nm) that could be due to the presence of the lowest concentration of Triacetin (12% w/w) in N1. The PI of CSB-INH nanoemulsions (N1–N5) was observed in the range of 0.189–0.324 (Table 3). The PI of nanoemulsions N1–N3 was relatively low (0.189–0.212), indicating good uniformity in droplet size as compared to nanoemulsions N4 and N5. Nanoemulsion N1 showed the least PI value (0.189), suggesting highest uniformity. However, the highest PI value was observed in nanoemulsion N5 (0.324).

The ZP values of CSB-INH nanoemulsions (N1–N5) were observed in the range of −42.6 to −30.8 mV (Table 3). The lowest value of ZP was observed in nanoemulsion N5 (−42.6 mV). However, the highest one was observed in nanoemulsion N1 (−30.8 mV). The negative net charge on ZP for all CSB-INH nanoemulsions was possibly due to the presence of fatty acid esters in Triacetin in all nanoemulsions as reported previously in the literature [34].

The viscosity of CSB-INH nanoemulsions (N1–N5) was observed in the range of 29.6–72.3 cP (Table 3). The viscosity of prepared nanoemulsions was also found to be reduced rapidly by decreasing the concentration of oil phase in nanoemulsions. The lowest viscosity was observed in nanoemulsion N1 (29.6 ± 2.7 cP) which was probably due to its lowest droplet size. However, the highest viscosity was observed in nanoemulsion N5 (72.3 ± 7.4 cP) due to its largest droplet size. The % T of CSB-INH nanoemulsions (N1–N5) was observed in the range of 96.1–98.9% (Table 3). The highest % T was observed in nanoemulsion N1 (98.9 ± 0.4%). However, the lowest one was observed in nanoemulsion N5 (96.1 ± 0.4%). The results of % T measurements showed the transparent nature of all nanoemulsions.

TEM analysis was performed to evaluate the surface morphology and shape of droplets of optimized nanoemulsion N1. TEM Photomicrographs of optimized nanoemulsion N1 were taken and interpreted (Fig. 2). The size of all droplets of nanoemulsion N1 was found to be less than 50 nm (Fig. 2). The shape of nanoemulsion droplets was observed as non-spherical (ovoidal) which was probably due to the presence of Triacetin and Tween-80 as reported by Anwer et al. (2014) [34]. The droplet size distribution of optimized nanoemulsion N1 recorded by TEM was in good agreement with the droplet size distribution recorded by scattering technique (Malvern Particle Size Analyzer).

3.5. In vitro drug release studies

In vitro drug release studies were performed via dialysis membrane on CSB-INH nanoemulsions (N1–N5) and drug suspension in order to get optimized nanoemulsion. The results of CSB-INH release from nanoemulsions and drug suspension are presented in Fig. 3. The initial release profile of CSB-INH from all nanoemulsions and drug suspension was found to be rapid (immediate type). The difference in the release profile of CSB-INH between nanoemulsions (N1–N5) and suspension is highly significant ($P < 0.05$). More than 50% of CSB-INH was found to be released from all nanoemulsions as compared to 15% from suspension formulation after 8 h of study (Fig. 3). After 8 h, all nanoemulsions and suspension formulation showed a slower release of CSB-INH (sustained release profile). The highest drug release profile of CSB-INH was observed in nanoemulsion N1 (Fig. 3). The cumulative % amount of CSB-INH that was released from N1 after 24 h was found to be 96.2% as compared to only 20.8% from suspension formulation. More than 85% of CSB-INH was released from N1 after 8 h of study. These results were in good agreement with the physicochemical characterization of nanoemulsions. The highest release profile of CSB-INH from N1 was possibly due to its lowest droplet size, lowest viscosity, least PI, highest % T and the presence of lowest concentration of oil phase (Triacetin). Two steps release profile of CSB-INH from developed nanoemulsions and suspension formulation indicated diffusion controlled dissolution rate of CSB-INH from all formulations [28].

3.6. Kinetic analysis of drug release data

In order to evaluate the accurate drug release mechanism, zero order, first order, Higuchi and Hixson–Crowel models were selected. Because, the drug release was significant for up to 8 h from all formulations, kinetic analysis was performed for up to 8 h drug release data. The results of release kinetic parameters are listed in Table 4. The release from all nanoemulsions (N1–N5) and suspension formulation followed the Peppas model with non-Fickian diffusion mechanism (Table 4). According to the Peppas model, If the value of n is equal to 0.5, the release mechanism is considered as diffusion controlled drug release (Fickian mechanism). However, if the value of n is greater than 0.5 but less than 1.0, the release mechanism is considered as non-Fickian diffusion mechanism. On the other hand, the value of n greater than 1.0 is related with supercase II transport mechanism [31]. The value of n in developed nanoemulsions (N1–N5) and suspension formulation was observed in the range of 0.877–0.982, indicating non-Fickian diffusion mechanism in all formulations. Our results of kinetic analysis were in good agreement with previous literature [35,36]. Based on lowest droplet size, least PI, lowest viscosity, optimal values of ZP & RI, highest % T, highest drug release profile and the presence of lowest concentration of Triacetin, CSB-INH nanoemulsion N1 was selected for further evaluation.

Table 3
Physicochemical characterization of CSB-INH nanoemulsions (N1–N5).

Code	Characterization parameters					
	Δ_{dm} ± SD (nm)	PI	ZP (mV)	η ± SD (cP)	RI ± SD	% T ± SD
N1	19.4 ± 2.3	0.189	−30.8	29.6 ± 2.7	1.341 ± 0.07	98.9 ± 0.4
N2	43.8 ± 4.6	0.209	−31.9	45.4 ± 3.8	1.342 ± 0.08	98.6 ± 0.3
N3	57.3 ± 6.3	0.212	−35.4	59.8 ± 4.9	1.344 ± 0.09	97.7 ± 0.2
N4	104.2 ± 9.7	0.312	−40.3	65.4 ± 6.2	1.346 ± 0.10	96.4 ± 0.5
N5	124.4 ± 14.8	0.324	−42.6	72.3 ± 7.4	1.347 ± 0.11	96.1 ± 0.4

Mean droplet diameter (Δdm), polydispersity index (PI), viscosity (η), % transmittance (% T), zeta potential (ZP), refractive index (RI), and standard deviation (SD).

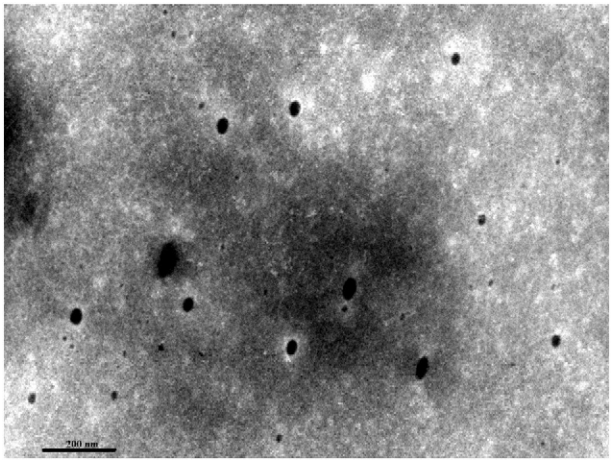

Fig. 2. Transmission electron microscopic (TEM) image of optimized CSB-INH nanoemulsion (N1) showing non-spherical droplets within submicrone range.

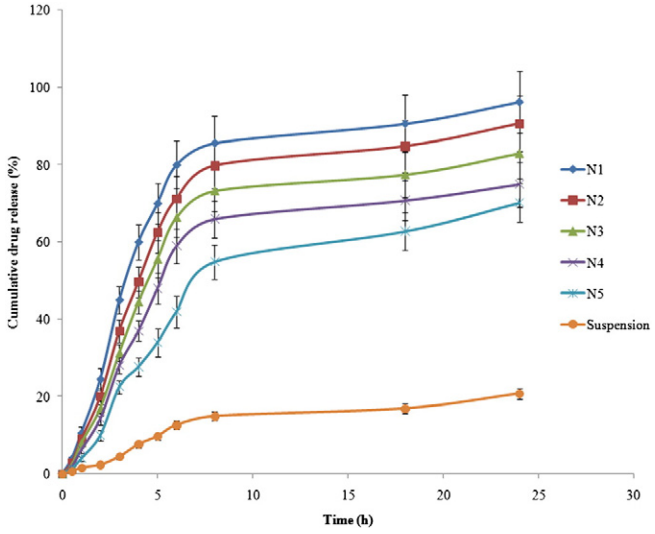

Fig. 3. In vitro drug release profile of CSB-INH from different nanoemulsions (N1–N5) and drug suspension via dialysis membrane.

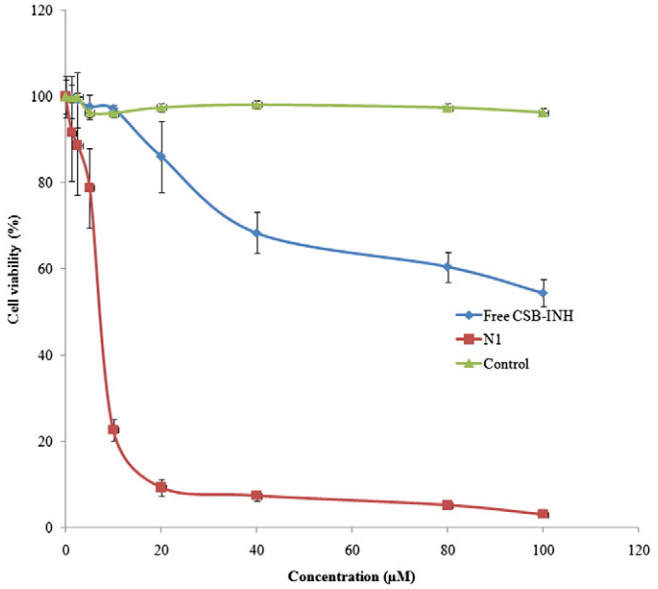

Fig. 4. Cell viability of CSB-INH in aqueous solution (free CSB-INH), control and optimized nanoemulsion N1 on HT-29 human colon cancer cell lines.

3.7. In vitro cytotoxic studies

Cell survival (%) was measured at 1.25, 2.5, 5, 10, 20, 40, 80 and 100 μM concentration of CSB-INH in an aqueous solution and N1 (Fig. 4). The highest cytotoxicity of free CSB-INH was observed as 45.60 ± 4.32% at a molar concentration of 100 μM (Table 5). However, the same molar concentration of CSB-INH in optimized nanoemulsion N1 showed 96.90 ± 6.02% cytotoxicity which was highly significant than free CSB-INH ($P < 0.05$). The lowest molar concentration (1.25 μM) of CSB-INH in N1 showed 8.42 ± 1.60% cytotoxicity as compared to only 0.14 ± 0.03% cytotoxicity of free CSB-INH (Table 5). Overall, CSB-INH in the form of nanoemulsion was found to be highly potent and efficacious than free CSB-INH on human colon cancer cell line. These results indicated the suitability of developed nanoemulsion in the treatment of colon cancer. The % viability of cells treated with free CSB-INH was found to be 54.40% at a molar concentration of 100 μM (Fig. 4). However, CSB-INH loaded nanoemulsion N1 showed significant growth inhibiting activity on the same cells. The cell viability of N1 treated cells was found to be only 3.10% at a molar concentration of 100 μM which was highly significant than free CSB-INH ($P < 0.05$). These results indicated the superiority of developed nanoemulsion as compared to free CSB-INH. On the other hand, control formulation did not inhibit cell growth at a greater extent (Fig. 4) which indicated that developed nanoemulsion components were nontoxic. The concentrations of free CSB-INH and N1 leading to 50% cell death (IC_{50}) were also determined by interpolation of concentration dependent cell viability curves (Fig. 4). The IC_{50} value of free CSB-INH was found to be 100.72 μM. However, the IC_{50} value of CSB-INH in N1 was found to be much lower than free CSB-INH (9.15 μM). Based on IC_{50} values, the CSB-INH in developed nanoemulsion was found to be around 9 times more efficacious than free CSB-INH which could reduce the dose of CSB-INH as well as its gastrointestinal adverse effects. Schiff bases have been investigated as good ligands for metals, hence the purported mechanism of action of CSB-INH could possibly be based on the formation of metal complexes which are known to inactivate the enzymes responsible for abnormal cell growth [37,38]. These results indicated that developed nanoemulsion of CSB-INH could be administered orally for the treatment of colon cancer.

3.8. Pharmacokinetic study in rats

The in vivo pharmacokinetic studies were performed to quantify CSB-INH in rat plasma after oral administration of CSB-INH nanoemulsion N1 and suspension formulation. The plasma concentration profiles of CSB-INH in adult male albino Wistar rats following oral administration of the optimized nanoemulsion (N1) and suspension formulation were compared. The plasma concentration profile of CSB-INH for optimized nanoemulsion represents a significantly greater improvement of CSB-INH oral absorption than suspension formulation (Fig. 5). The results of pharmacokinetic parameters of N1 and drug suspension are listed in Table 6. The T_{max} was observed as 1.5 h for N1 and as well as for suspension formulation. However, the C_{max} of N1 was found to be 452.19 ng/ml as compared to 210.89 ng/ml of suspension formulation. Statistically, the difference in C_{max} of N1 was highly significant ($P < 0.001$) as compared to suspension formulation. It was also observed that AUC_{0-t} and $AUMC_{0-t}$ of N1 were 1313.73 and 3870.57 ng·h/ml, respectively, which were highly significant ($P < 0.001$) as compared to AUC_{0-t} (618.69 ng·h/ml) and $AUMC_{0-t}$ (2048.08 ng·h/ml) of suspension formulation.

Table 4
Correlation coefficients and release rate constants of CSB-INH nanoemulsions (N1—N5) and drug suspension.

Formulation	Zero order		First order		Higuchi	Hixson–Crowell	Peppas	
	K_0	R^2	k_1	R^2	R^2	R^2	R^2	n
N1	11.86	0.939	1.866	0.971	0.978	0.981	0.979	0.982
N2	11.06	0.964	1.659	0.968	0.982	0.989	0.983	0.980
N3	10.28	0.969	1.531	0.934	0.978	0.985	0.981	0.962
N4	9.25	0.976	1.412	0.959	0.976	0.985	0.985	0.943
N5	7.31	0.983	1.270	0.988	0.972	0.993	0.988	0.877
Suspension	2.06	0.981	1.051	0.978	0.943	0.977	0.985	0.897

Correlation coefficient (R2), zero order rate constant (K0), first order rate constant (k1), and diffusion coefficient (n).

Table 5
Cytotoxicity (%) of free CSB-INH, optimized nanoemulsion (N1) and control on HT-29 human colon cancer cell lines ($n = 3$).

Concentration (μM)	Cytotoxicity (% ± SD)		
	Free CSB-INH	N1	Control
0	0	0	0
1.25	0.14 ± 0.03	8.42 ± 1.60	0.29 ± 0.04
2.50	0.75 ± 0.07	11.28 ± 1.89	0.11 ± 0.02
5.00	2.38 ± 0.11	21.16 ± 2.46	3.72 ± 0.16
10.00	2.73 ± 0.14	77.28 ± 5.27	3.86 ± 0.21
20.00	13.89 ± 1.53	90.62 ± 6.20	2.52 ± 0.31
40.00	31.62 ± 2.20	92.52 ± 7.12	1.87 ± 0.10
80.00	39.55 ± 3.56	94.80 ± 5.74	2.60 ± 0.42
100.00	45.60 ± 4.32	96.90 ± 6.02	3.70 ± 0.54

However, the difference in the values of MRT was not statistically significant ($P > 0.05$) when the nanoemulsion and suspension formulations were compared. The relative bioavailability of N1 with respect to suspension formulation was observed as 212.34%. The absorption of CSB-INH from optimized nanoemulsion N1 resulted in a 2.12fold increase in bioavailability as compared to suspension formulation. The enhanced bioavailability of CSB-INH from nanoemulsion was probably due to lower droplet size, higher drug release and the presence of surfactants such as Tween-80 and Transcutol-HP in the formulations [26].

4. Conclusions

In the present study, the carvone Schiff base of isoniazid was synthesized and characterized for its possible anticancer potential. Various nanoemulsion formulations of CSB-INH were developed, characterized, and evaluated for in vitro cytotoxicity and in vivo pharmacokinetic studies. Based on the lowest droplet size (19.4 nm), least PI (0.189), lowest viscosity (29.6 cP), optimal values of ZP (−30.8 mV) & RI (1.341), highest % T (98.9%), highest drug release profile (94.5% after 24 h) and the presence of the lowest concentration of Triacetin (12% w/w), CSB-INH nanoemulsion N1 was selected for in vitro cytotoxicity and in vivo pharmacokinetic studies. In vitro cytotoxicity studies on HT-29 human colon cancer cells indicated that CSB-INH in optimized nanoemulsion was around seven times more efficacious than free CSB-INH in terms of cell growth inhibiting activity. Moreover, pharmacokinetic studies in rats showed rapid absorption of CSB-INH from optimized nanoemulsion as compared to its suspension formulation. The oral bioavailability of CSB-INH was significantly higher than its suspension formulation. From

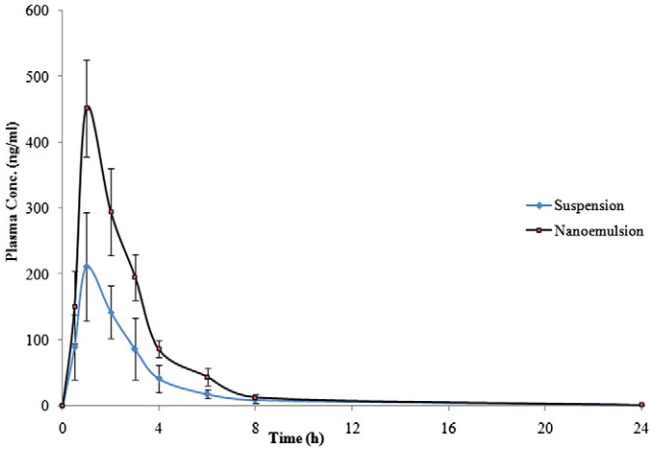

Fig. 5. Plasma concentration–time profile curves of CSB-INH after oral administration of optimized nanoemulsion and suspension formulations in adult male Albino rats (Mean ± SD, n = 6 and dose 5 mg/kg).

Table 6
Pharmacokinetic parameters (mean ± SE, n = 6) of CSB-INH after an oral administration of optimized nanoemulsion (N1) and CSB-INH suspension (5 mg/kg).

Parameters	CSB-INH suspension (Mean ± SE)	CSB-INH nanoemulsion (Mean ± SE)
C_{max} (ng/ml)	210.89 (61.28)	452.19 (55.64)***
T_{max} (h)	1.5	1.5
AUC_{0-24} (ng·h/ml)	618.69 (164.90)	1313.73 (138.97)***
$AUMC_{0-24}$ (ng·h/ml)	2048.08 (512.74)	3870.57 (664.78)***
λz (h^{-1})	0.18 (0.01)	0.20 (0.01)
$T_{½}$ (h)	3.82 (0.27)	3.47 (0.18)
MRT (h)	3.34 (0.24)	2.96 (0.32)
Relative bioavailability (%)	100	212.34

*p < 0.01 significant, ***p < 0.001) highly significant compared to CSB-INH suspension.

these results, it was concluded that the developed nanoemulsion might be a promising vehicle for oral delivery of CSB-INH for the treatment of colon cancer. For definitive preclinical results, further in vivo studies will be performed in an appropriate animal colon cancer model to ascertain efficacy in terms of reduction in tumor size.

Conflict of interest

The authors declare that they have no conflict of interest.

Acknowledgment

The authors would like to extend their sincere appreciation to the Deanship of Scientific Research and Research Center, College of Pharmacy, King Saud University.

References

[1] H.S.N. Kumar, T. Parumasivam, F. Jumaat, P. Ibrahim, M.Z. Asmawi, A. Sadikun, Synthesis and evaluation of isonicotinoyl hydrazone derivatives as antimycobacterial and anticancer agents, Med. Chem. Res. 23 (2014) 269–279.
[2] O.H. Sjo, M. Berg, M. Merok, M. Kolberg, A. Svindland, R.A. Lothe, A. Nesbakken, Peritoneal carcinomatosis of colon cancer origin: highest incidence in women and in patients with right-sided tumors, J. Surg. Oncol. 104 (2011) 792–797.
[3] P. Yin, Y. Wang, Y. Qiu, L. Hou, X. Liu, J. Qin, Y. Duan, P. Liu, M. Qiu, Q. Li, Bufalin-loaded mPEG-PLGA-PLL-cRGD nanoparticles: preparation, cellular uptake, distribution and anticancer activity, Int. J. Nanomedicine 7 (2012) 3961–3969.
[4] D.M. Parkin, F. Bray, J. Ferlay, P. Pisani, Global cancer statistics, 2002, CA Cancer J. Clin. 55 (2005) 74–108.
[5] Z. Rahman, K. Kohli, R.K. Khar, M. Ali, N.A. Charoo, A.A. Shamsher, Characterization of 5-fluorouracil microspheres for colonic delivery, AAPS PharmSciTech 7 (2006) E47.
[6] M.A. Bhat, M.A. Al-Omar, Synthesis, characterization and in vitro anti-*Mycobacterium tuberculosis* activity of terpene Schiff bases, Med. Chem. Res. 22 (2013) 4522–4528.
[7] N. Demirbas, S.A. Karaoglu, A. Demirbas, K. Sancak, Synthesis and antimicrobial activities of some new 1-(5-phenylamino-[1,3,4] thiadiazol-2-yl) methyl-5-oxo-[1,2,4] triazole and 1-(4-phenyl-5-thioxo-[1,2,4] triazol-3-yl) methyl-5-oxo-[1,2,4] triazolederivatives, Eur. J. Med. Chem. 39 (2004) 793–804.
[8] P. Vicini, M. Incerti, I.A. Doytchinova, P. La Colla, B. Busonera, R. Loddo, Synthesis and anti proliferative activity of benzo[d]isothiazole hydrazones, Eur. J. Med. Chem. 41 (2006) 624–632.
[9] K. Sztanke, T. Tuzimski, J. Rzymowska, K. Pasternak, A.M. Kandefer-Szersze, Synthesis, determination of the lipophilicity, anticancer and antimicrobial properties of some fused 1,2,4-triazole derivatives, Eur. J. Med. Chem. 43 (2008) 404–419.
[10] T.J. de Faria, M. Roman, N.M. de Souza, R.D. Vecchi, J.V. de Assis, A.L.G. dos Santos, I.H. Bechtold, N. Winter, M.J. Soares, L.P. Silva, M.V. De Almeida, A. Bafica, An isoniazid analogue promotes *Mycobacterium tuberculosis*-nanoparticle interactions and enhances bacterial killing by macrophages, Antimicrob. Agents Chemother. 56 (2012) 2259–2267.
[11] F.A.R. Rodrigues, A.C.E. Oleveira, B.C. Cavalcanti, C. Pessoa, A.C. Pinheiro, M.N.V. De Souza, Biological evaluation of isoniazid derivatives as an anticancer class, Sci. Pharm. 82 (2014) 21–28.
[12] H. Kumar, D. Malhotra, R. Sharma, E. Sausville, M. Malhotra, Synthesis, characterization and evaluation of isoniazid analogues as potent anticancer agents, Pharmacologyonline 3 (2011) 337–343.
[13] F.K. Alanazi, N. Haq, A.A. Radwan, I.A. Alsarra, F. Shakeel, Formulation and evaluation of cholesterol-rich nanoemulsion (LDE) for drug delivery potential of cholesteryl-maleoyl-5-fluorouracil, Pharm. Dev. Technol. 20 (2015) 266–270.
[14] F.K. Alanazi, N. Haq, A.A. Radwan, I.A. Alsarra, F. Shakeel, Cholesterol-rich nanoemulsions (LDE) for drug targeting of cholesteryl-succinyl-5-fluorouracil conjugate, Curr. Nanosci. 10 (2014) 287–291.

[15] F. Shakeel, N. Haq, A. Al-Dhfyan, F.K. Alanazi, I.A. Alsarra, Chemoprevention of skin cancer using low HLB surfactant nanoemulsion of 5-fluorouracil: a preliminary study, Drug Deliv. (2013). http://dx.doi.org/10.3109/10717544.2013.868557.
[16] J.A. Moura, C.J. Valduga, E.R. Tavares, I.F. Kretzer, D.A. Maria, R.C. Maranhão, Novel formulation of a methotrexate derivative with a lipid nanoemulsion, Int. J. Nanomedicine 6 (2011) 2285–2295.
[17] C.H. Azevedo, J.P. Carvalho, C.J. Valduga, R.C. Maranhão, Plasma kinetics and uptake by the tumor of a cholesterol-rich microemulsion (LDE) associated to etoposide oleate in patients with ovarian carcinoma, Gynecol. Oncol. 97 (2005) 178–182.
[18] D.G. Rodrigues, D.A. Maria, D.C. Fernandes, C.J. Valduga, R.D. Couto, O.C.M. Ibanez, R.C. Maranhao, Improvement of paclitaxel therapeutic index by derivatization and association to a cholesterol-rich microemulsion: in vitro and in vivo studies, Cancer Chemother. Pharmacol. 55 (2005) 565–576.
[19] M.L. Dias, J.P. Carvalho, D.G. Rodrigues, S.R. Graziani, R.C. Maranhão, Pharmacokinetics and tumor uptake of a derivatized form of paclitaxel associated to a cholesterol-rich nanoemulsion (LDE) in patients with gynecologic cancers, Cancer Chemother. Pharmacol. 59 (2007) 105–111.
[20] R. Pandey, A. Zahoor, S. Sharma, G.K. Khuller, Nanoparticle encapsulated antitubercular drugs as a potential oral drug delivery system against murine tuberculosis, Tuberculosis 83 (2003) 373–378.
[21] A. Sharma, R. Pandey, S. Sharma, G.K. Khuller, Chemotherapeutic efficacy of poly(dl-lactide-co-glycolide) nanoparticle encapsulated antitubercular drugs at subtherapeutic dose against experimental tuberculosis, Int. J. Antimicrob. Agents 24 (2004) 599–604.
[22] P. Blasi, A. Schoubben, S. Giovagnoli, C. Rossi, M. Ricci, Fighting tuberculosis: old drugs, new formulations, Expert Opin. Drug Deliv. 6 (2009) 977–993.
[23] A. Sosnik, A.M. Carcaboso, R.J. Glisoni, New old challenges in tuberculosis: potentially effective nanotechnologies in drug delivery, Adv. Drug Deliv. Rev. 62 (2010) 547–559.
[24] R. Pandey, Z. Ahmad, Nanomedicine and experimental tuberculosis: facts, flaws, and future, Nanomedicine 7 (2011) 259–272.
[25] A. Dorhoi, S.T. Reece, S.H. Kaufmann, For better or for worse: the immune response against *Mycobacterium tuberculosis* balances pathology and protection, Immunol. Rev. 240 (2011) 235–251.
[26] S. Shafiq, F. Shakeel, S. Talegaonkar, F.J. Ahmad, R.K. Khar, M. Ali, Development and bioavailability assessment of ramipril nanoemulsion formulation, Eur. J. Pharm. Biopharm. 66 (2007) 227–243.
[27] F. Shakeel, S. Shafiq, N. Haq, F.K. Alanazi, I.A. Alsarra, Nanoemulsions as potential vehicles for transdermal and dermal delivery of hydrophobic compounds: an overview, Expert Opin. Drug Deliv. 9 (2012) 953–974.
[28] F. Shakeel, N. Haq, M. Elbadry, F.K. Alanazi, I.A. Alsarra, Ultra fine super selfnanoemulsifying drug delivery system (SNEDDS) enhanced solubility and dissolution of indomethacin, J. Mol. Liq. 180 (2013) 89–94.
[29] F. Shakeel, N. Haq, F.K. Alanazi, I.A. Alsarra, Impact of various nonionic surfactants on self-nanoemulsification efficiency of two grades of Capryol (Capryol-90 and Capryol-PGMC), J. Mol. Liq. 182 (2013) 57–63.
[30] H. Yu, Q. Huang, Improving the oral bioavailability of curcumin using novel organogel-based nanoemulsions, J. Agric. Food Chem. 60 (2012) 5373–5379.
[31] P. Costa, J.M.S. Lobo, Modeling and comparison of dissolution profiles, Eur. J. Pharm. Sci. 15 (2001) 123–133.
[32] S. Dash, P.N. Murthy, L. Nath, P. Chowdhury, Kinetic modeling on drug release from controlled drug delivery systems, Acta Pol. Pharm. 67 (2010) 217–223.
[33] M. Iqbal, M.A. Bhat, F. Shakeel, Development and validation of UHPLC-MS/MS assay for rapid determination of a carvone Schiff base of isoniazid (CSB-INH) in rat plasma: application to pharmacokinetic study, Biomed. Chromatogr. (2014). http://dx.doi.org/10.1002/bmc.3368.
[34] M.K. Anwer, S. Jamil, E.O. Ibnouf, F. Shakeel, Enhanced antibacterial effects of clove essential oil by nanoemulsion, J. Oleo Sci. 63 (2014) 347–354.
[35] O. Nuchuchua, U. Sakulku, N. Uawongyart, S. Puttipipatkhachorm, A. Soottitantawat, N. Ruktanonchai, In vitro characterization and mosquito (*Aedes aegypti*) repellent activity of essential-oils-loaded nanoemulsions, AAPS PharmSciTech 10 (2009) 1234–1242.
[36] M. El-Badry, N. Haq, G. Fetih, F. Shakeel, Solubility and dissolution enhancement of tadalafil using self-nanoemulsifying drug delivery system, J. Oleo Sci. 63 (2014) 567–576.
[37] A. Kajal, S. Bala, S. Kamboj, N. Sharma, V. Saini, Schiff base: a versatile pharmacophore, J. Catal. 2013 (2013) (E893512).
[38] A.J. Guo, X.S. Xu, Y.H. Hu, M.Z. Wang, X. Tan, Effects of ternary complexes of copper with salicylaldihyde-amino acid Schiff base coordination compounds on the proliferation of BGC823 cells, Chin. J. Cancer 29 (2010) 277–282.